Materials Transactions, Vol. 45, No. 7 (2004) pp. 2326 to 2331

In-situ Observation of Growth Behavior of Fe-Zn Intermetallic Compounds at Initial Stage of Galvannealing Process

Akira Taniyama[1], Masahiro Arai[1], Toru Takayama[1] and Masugu Sato[2]

[1]*Corporate Research and Development Laboratories, Sumitomo Metal Industries, Ltd., Amagasaki 660-0891, Japan*
[2]*Japan Synchrotron Radiation Research Institute, Mikazuki-cho, Hyogo 679-5198, Japan*

In-situ observation was performed with X-ray diffraction technique using synchrotron radiation to reveal growth behavior of the Fe-Zn intermetallic compounds, the ζ and δ_1 phases, at the initial stage of galvannealing process. The galvanized sample and electroplated sample were used in the observation. The diffraction peak profiles were successfully obtained at intervals of 1 second with heating the sample, and the growth of the Fe-Zn intermetallic compounds was observed dynamically. In the galvanized sample including a small amount of aluminum in the coating, there was an incubation period of 7 seconds before the δ_1 phase started to grow. The thickness estimated with the peak intensity of the δ_1 phase increased in proportion to the square root of heating time when the incubation period was taken into account. In the electroplated sample including no aluminum in the coating, the thickness of ζ phase increased in proportion to the square root of heating time. The δ_1 phase started to grow as soon as the ζ phase occupied the entire coating. The thickness of the δ_1 phase also increased in proportion to the square root of heating time. These results suggest that that the growth behavior of the δ_1 phase at the initial stage of galvannealing is dominated by the interdiffusion between Fe and Zn, neither by interfacial reaction nor by autocatalytic reaction whether the coating contains aluminum or not.

(Received March 5, 2004; Accepted May 27, 2004)

Keywords: *galvannealing, iron-zinc intermetallic compound, growth behavior, in-situ observation, synchrotron radiation*

1. Introduction

Since a small amount of aluminum was added in molten zinc bath in the industrial galvanizing process in order to inhibit growth of the Fe-Zn intermetallic compounds in the bath, it is very important to understand the effect of aluminum in zinc coating on the growth behavior of the Fe-Zn during hot-dip galvanizing process. The inhibition mechanism has been understood that the Fe-Al layer formed at the interface between zinc coating and steel substrate as soon as the substrate was immersed in the bath, and the layer inhibits the Fe-Zn reaction between the zinc coating and the steel substrate.[1,2] Growth behavior of the Fe-Al layer depends on the temperature and aluminum concentration in the bath.[3,4] The Fe-Al layer also causes the occurrence of outburst structure, where the Fe-Zn layer has many cracks and liquid zinc penetrated.[5,6] It has been reported that the outburst structure effects on the growth behavior of Fe-Zn at the initial stage of galvannealing;[7,8] the Fe-Zn layer grows linearly with heating time at the initial stage, and then the growth of the thick Fe-Zn layer follows the parabolic law.[7] Furthermore, a similar result has been obtained in the experiment of galvannealing process.[8]

However, the growth behavior of the Fe-Zn during galvanizing or galvannealing process has been observed by static analyses such as a cross-sectional observation of the coating with an optical or electron microscope, and a measurement of iron contents in the coating using the samples quenched after annealing. In these analyses, it is very difficult to understand the growth behavior in detail because those reactions occur in a short period. Therefore, a rapid detection, *i.e.*, "*in-situ* observation" system is required to follow those reactions dynamically. The *in-situ* observation using X-ray diffraction method is a very useful technique to identify the Fe-Zn intermetallic compounds and to quantify their growth in the coating. In order to perform the *in-situ* observation of the growth behavior of the Fe-Zn in the coating, penetration length of X-ray and time definition of detector are important factors because it is necessary to observe the whole of coating having 10~20 μm thickness, and to observe the rapid reaction. Although it is an easy way for achieving good time definition of detector to increase the intensity of source, it is very difficult for a conventional X-ray source to obtain enough intensity for the *in-situ* observation. Therefore, synchrotron radiation, which has higher energy and higher intensity than those of the conventional X-ray source, is necessary for the *in-situ* observation as an X-ray source. Recently, some synchrotron radiation experiments applied to an observation of the Fe-Zn reaction has been reported.[9–11]

In this study, the *in-situ* observation of the growth of the Fe-Zn intermetallic compounds in the zinc coating during galvannealing process was performed with X-ray diffraction method using synchrotron radiation. In the experiment, a time dependency of diffraction profiles was detected quantitatively with galvanized samples including aluminum in the coating and electroplated samples including no aluminum in the coating. The growth behavior of the δ_1 and ζ phase in the coating at the initial stage of the galvannealing process was discussed with the quantitative results of their growth. Furthermore, the effect of aluminum in the coating on the growth behavior was also discussed.

2. Experimental Procedure

2.1 Preparation of zinc plated samples

Two kinds of samples were prepared in this study, one had a zinc coating containing a small amount of aluminum and the other had a pure zinc coating. They were plated by means of a galvanizing method and an electroplating method, hereafter; they are called the galvanized sample and the electroplated sample, respectively. The cold-rolled interstitial-free (IF) steel sheets were used as substrates. The chemical composition of the IF steel is shown in Table 1.

Table 1 Chemical composition of IF steel sheet (mass%).

C	Si	Mn	P	S	sol. Al	Ti
0.003	0.01	0.08	0.012	0.007	0.042	0.022

They were annealed at 1053 K in the 10%H_2-N_2 atmosphere just before the galvanizing or the electroplating. The galvanizing was conducted with dipping the steel sheets in a molten zinc bath containing 0.13 mass% Al and saturated with iron, for 1 second at 733 K, using a hot-dip galvanizing simulator. The dipped steel sheets were cooled in a N_2 atmosphere at the cooling rate of 5 K/s. The electroplating was conducted with the electrolyte solution containing 400 g $ZnSO_4 \cdot 7H_2O$ and 75 g Na_2SO_4 in 1 dm^3 of water. The pH of the solution was adjusted to 2 by adding H_2SO_4. A plate of zinc was used as an anode. The current density was 1000 Am^{-2}. The samples had the zinc coatings of 10 µm in thickness. They were stamped out to be disks of 14 mm in diameter. One side of the disk was polished to remove the coating.

2.2 *In-situ* X-ray diffraction measurement with synchrotron radiation

The synchrotron radiation experiments were performed at BL19B2 in SPring-8. Figure 1 shows a schematic illustration of the *in-situ* observation system. The infrared heater designed for the observation was mounted on the 8-axes goniometer of diffractometer. The sample was laid on a quartz holder its coating side down in the sample chamber filled with N_2 gas, and was heated from its polished side. The sample temperature was measured at the upper surface and the lower surface. Taking account of the thickness of the coating and the necessary resolution of the scattering vector, the wavelength of X-ray was chosen to be 0.0443 nm. The size of incident X-ray was 5 mm in width × 0.1 mm in height. An incident angle of the X-ray was kept 5 degrees from the surface of the specimen. An imaging plate (Fuji Film, BAS-MS2040: 50 µm/pixel) was used as a sensitive 2D X-ray detector to obtain a time dependence of diffraction profiles. A receiving slit of 2.5 mm width was mounted in front of the imaging plate. In order to obtain diffraction profiles every second, the imaging plate was scanned at 2.5 mm/s during the

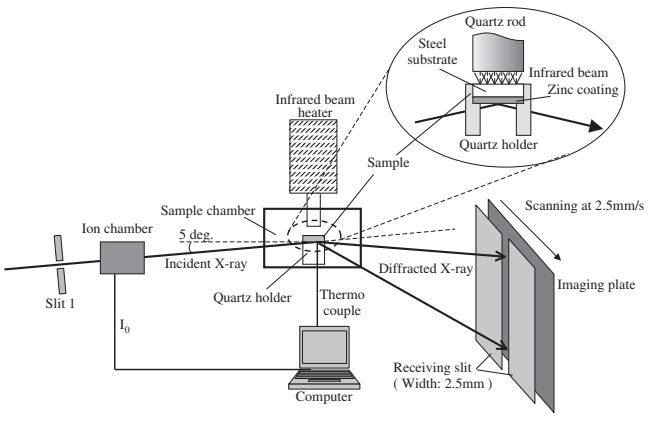

Fig. 1 Schematic illustration of *in-situ* observation system with synchrotron radiation.

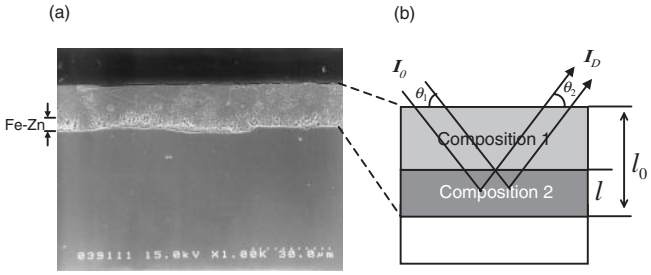

Fig. 2 Schematic illustration of layered model for estimating the thickness of Fe-Zn. (a) Cross-sectional SEM image of the quenched galvanized sample after annealed for 20 seconds at 733 K. (b) Layered model for the estimation.

measurement. The exposed imaging plates were read out with an IP-reader (Fuji Film, BAS2500) after waiting for 30 minutes with taking a fading effect into account.[12)]

2.3 Estimating method of thickness of Fe-Zn intermetallic compound

From the several cross sectional observations of zinc coating using samples quenched in water during galvannealing process, it has been understood that the Fe-Zn intermetallic compound grows from the vicinity of the interface between zinc coating and steel substrate as shown in Fig. 2(a). Therefore, the effect of absorption of X-ray should be taken into account in the estimation of thickness of the Fe-Zn intermetallic compound. Although the Fe-Zn layer has roughness in a microscopic viewpoint, the layer can be considered to be a uniform layer in macroscopic viewpoint such as X-ray diffraction method. Therefore, the layered structure model shown in Fig. 2(b) was used in the estimation.

The intensity ratio of diffracted X-ray from the Fe-Zn layer is expressed by the following equation:

$$\frac{I_{\mathrm{D}}(l)}{I_{\mathrm{D}}(l_0)} = \exp(-\mu_1(l_0 - l)\beta)\frac{1 - \exp(-\mu_2 l\beta)}{1 - \exp(-\mu_2 l_0\beta)}, \quad (1)$$

where, the l_0 is the full thickness of coating. The $I_{\mathrm{D}}(l)$ is the intensity of diffraction peak obtained from the composition 2 whose thickness has l. The μ_1 and μ_2 are linear absorption coefficients of the composition 1 and the composition 2, respectively. The volume density of the Fe-Zn in the layer was assumed to be constant. The β is expressed as follows,

$$\beta = \frac{1}{\sin\theta_1} + \frac{1}{\sin\theta_2}. \quad (2)$$

Here, the θ_1 is the angle between the incident X-ray and the surface of the sample, and the θ_2 is the angle between the diffracted X-ray and the surface. With the eq. (1) and (2), the $I_{\mathrm{D}}(l)$ obtained from the composition 2 is converted to its thickness l. In the galvannealing process, it is known that the Fe-Zn intermetallic compounds such as ζ ($FeZn_{13}$) and δ_1 ($FeZn_7$ or $FeZn_{10}$) phases.[13)] Although the linear absorption coefficient of the compound depends on its chemical composition, the coefficients for zinc and these Fe-Zn compounds were in the range from 108.9 to 110.1 cm^{-1}. In this study, it was assumed that they had the same linear absorption coefficients, and the coefficient for the ζ phase (109.3 cm^{-1}) was used.

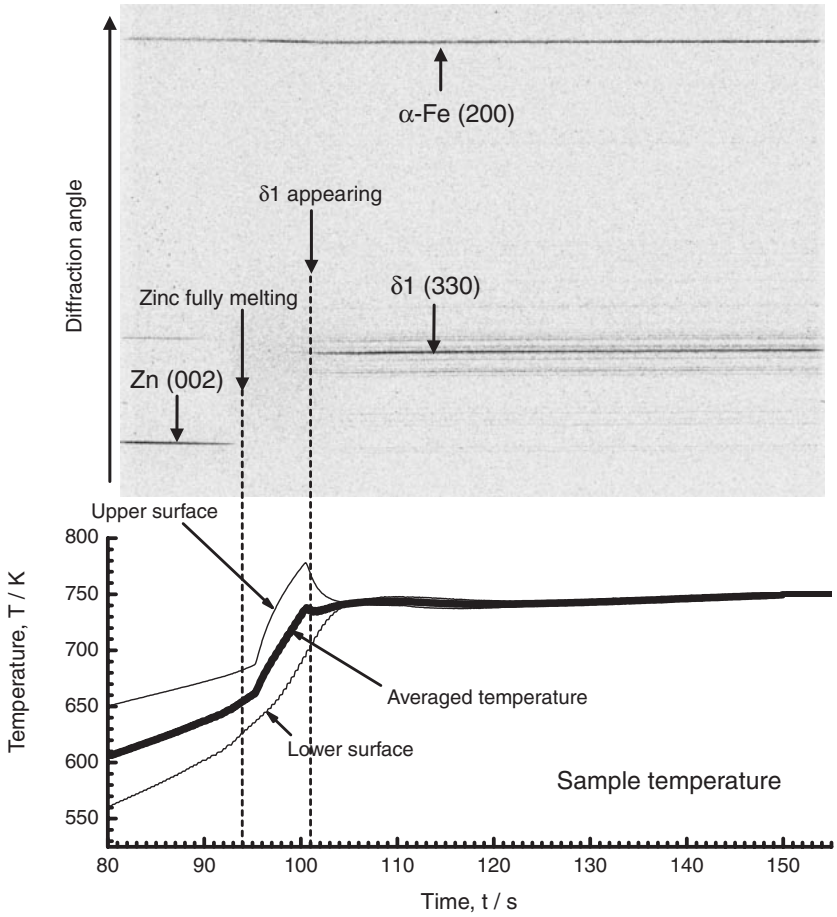

Fig. 3 Diffraction profile image recorded on an imaging plate and temperature profile of the galvanized sample.

3. Results and Discussion

3.1 Galvanized coating

Figure 3 shows the diffraction profile image recorded on an imaging plate during heat treatment at 733 K. The temperature profile of the sample is also shown in the figure. The heating rate up to 733 K was 15 K/s after the zinc coating fully melting. The diffracted X-ray was indicated as black lines on the image. The 200-diffraction peak of α-Fe obtained from the steel substrate was observed through the measurement. Therefore, the diffraction profile includes information about the entire zinc coating under this experimental condition. Since image intensity on an imaging plate has a linear relationship with intensity of irradiated X-ray, the peak intensity in the diffraction profile can be quantitatively obtained from the image intensity. Figure 4 shows the diffraction peak profiles extracted from the diffraction profile image. The time indicated in the figure started as soon as the zinc coating fully melted. A change of the diffraction peaks were successfully observed every second. Since the background noises in the peak profiles were on a very low level, weak diffraction peaks were well detected. In the profiles, no diffraction peak of the ζ phase was observed, and the 330-diffraction peak of the δ_1 phase was observed during the heat treatment. Figure 5(a) shows a relationship between the intensity of the 330-diffraction peak and the heating time. The intensity was normalized with the maximum of the peaks. No diffraction peak of the δ_1 phase was observed within 7 seconds after the zinc coating fully melted. This period is called an incubation period (t_{inc}). It is considered that the Fe-Al interfacial layer (Fe_2Al_5 or $FeAl_3$) causes the incubation period was because it inhibits the interdiffusion of iron and zinc between the zinc coating and the steel substrate.[1,2] Figure 5(b) shows a relationship between estimated thickness of the δ_1 phase and the heating time. It was found that thickness of the δ_1 phase increased in proportion to the square root of heating time when the incubation period was taken into account. Therefore, the thickness (l) is expressed by the following equation:

$$l = \sqrt{k \cdot (t - t_{inc})}, \tag{3}$$

where the k ($\mu m^2 s^{-1}$) is a growth rate constant, and the t is a heating time. The growth of the δ_1 phase was well fitted with the growth rate constant of 15.89 $\mu m^2 s^{-1}$ and the incubation period of 7.0 s. Figure 6 shows the comparison of growth behavior of the δ_1 phase in the coatings of 10 μm and 30 μm in thickness.[11] Although there is a little difference in the growth rate and the incubation period, the thickness of the δ_1 phase in both the coatings is plotted on the same parabola, approximately. This result suggests that the growth behavior of the δ_1 phase always follows parabolic law during galvannealing process.

The above results contradict the results proposed by Yamaguchi and Hisamatsu.[7] They measured iron quantity in the coating during immersion in the molten zinc bath including various aluminum contents, and discussed the

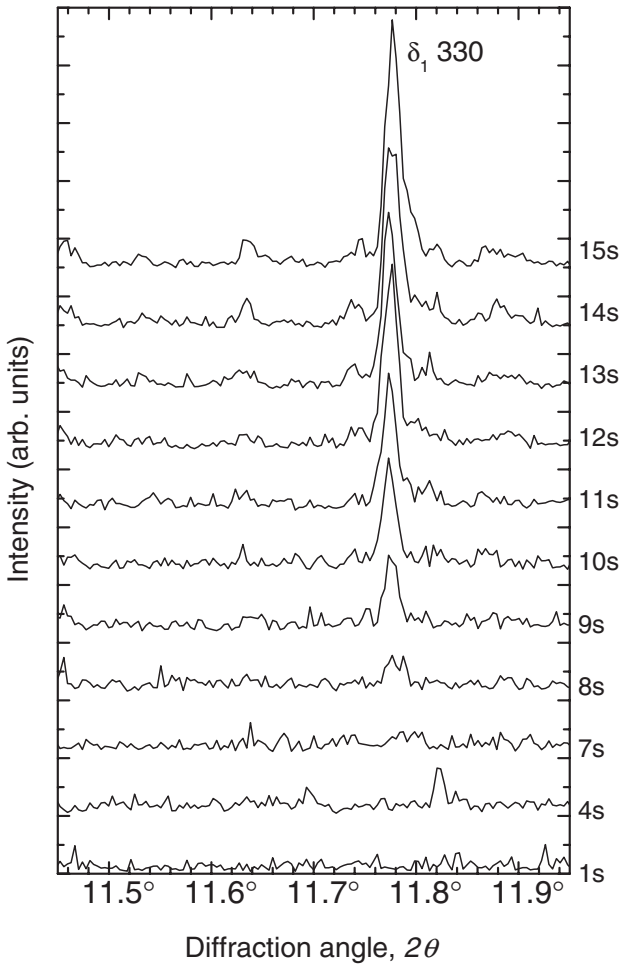

Fig. 4 Change of the diffraction profiles in the galvanized sample during heat treatment at 733 K.

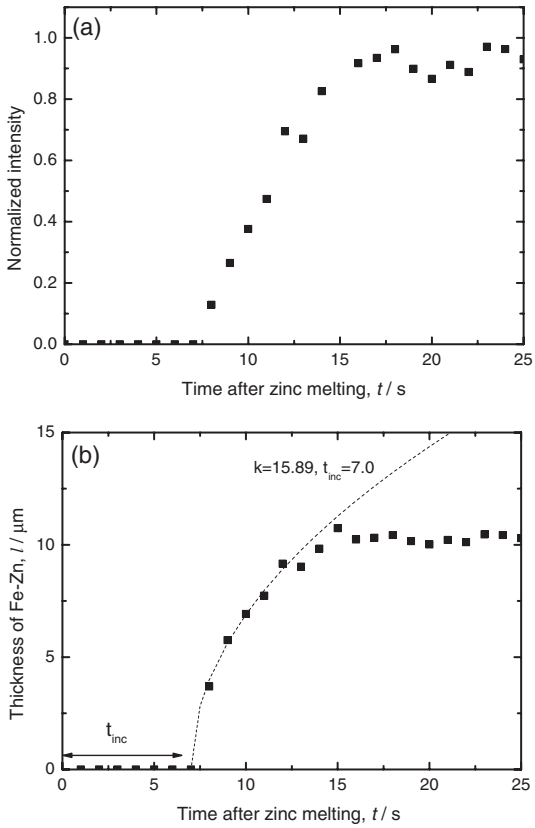

Fig. 5 Variations of the intensity of diffraction peak and the estimated thickness of the Fe-Zn intermetallic compound in the galvanized sample. (a) Intensity of the δ_1 330-diffraction peak (b) Thickness of the δ_1 phase.

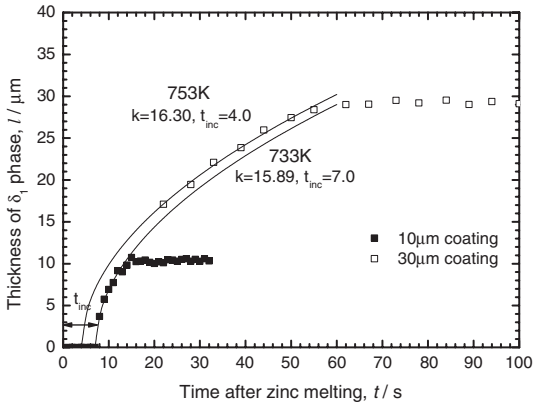

Fig. 6 Comparison of the variation of the δ_1 phase's thickness between thin and thick coating in the galvanized sample.

dependence of growth behavior of Fe-Zn on the aluminum content with the relationship between the iron quantity and the immersion time. They concluded that the outburst structure grows linearly with heating time at the initial stage of galvannealing process when the molten zinc bath including a small amount of aluminum and that the growth of the thick Fe-Zn layer follows the parabolic law. However, their results of the iron quantity at the initial stage follows the parabolic law when the incubation period is taken into account just as mentioned in this study since they also found the incubation period in the growth of the Fe-Zn. Therefore, it is concluded that the growth behavior of the δ_1 phase in the coating including a small amount of aluminum is dominated only by the interdiffusion between Fe and Zn atoms, neither by the interfacial reaction nor by the autocatalytic reaction, at the initial stage of galvannealing process.

3.2 Pure zinc coating

Figure 7 shows the diffraction profiles obtained from the electroplated sample during heat treatment at 733 K. The heating rate up to 733 K was 15 K/s after the zinc coating fully melting. In the profiles, the −312-diffraction peak of the ζ phase and the 330-diffraction peak of the δ_1 phase were observed. Figure 8(a) shows variations of the −312-diffraction peak intensity of the ζ phase and the 330-diffraction peak intensity of the δ_1 phase. The diffraction peak of the ζ phase appeared as soon as the zinc coating fully melted. No diffraction peak of the δ_1 phase was observed within 6 seconds after the zinc coating fully melted. Thus, an incubation period in the growth of the δ_1 phase was observed even in the electroplated sample. When the diffraction peak of the δ_1 phase appeared, the intensity of the diffraction peak of the ζ phase was just about to reach to the maximum. The intensity of the ζ phase decreased with increasing of the peak intensity of the δ_1 phase. This suggests that the δ_1 phase starts to grow as soon as the ζ phase occupies the entire coating. Figure 8(b) shows a relationship between the estimated thickness of the ζ and δ_1 phases in the coating and the heating

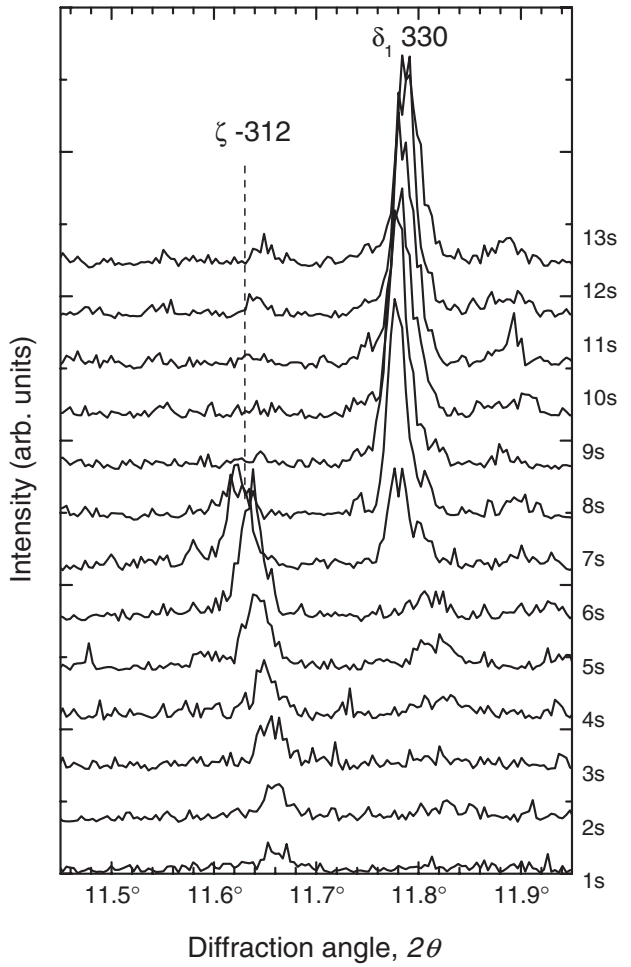

Fig. 7 Change of the diffraction profiles in the electroplated sample during heat treatment at 733 K.

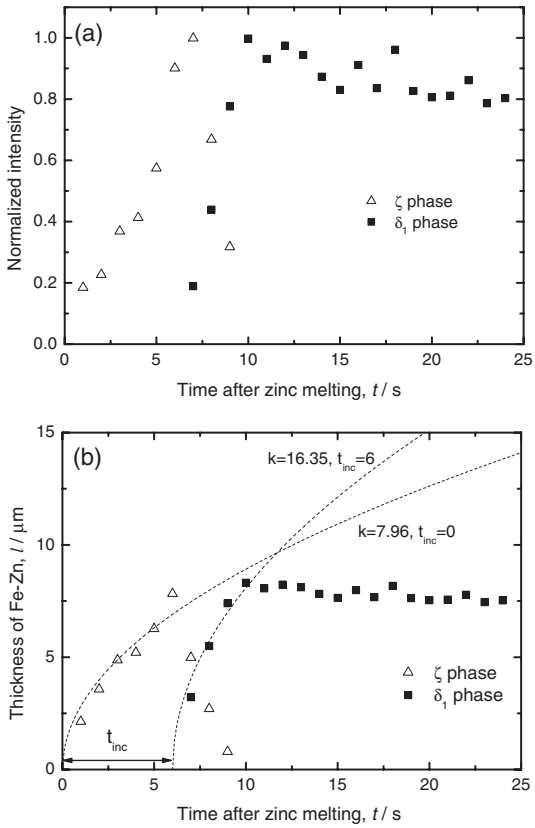

Fig. 8 Variations of the intensity of diffraction peak and the estimated thickness of the Fe-Zn intermetallic compound in the electroplated sample. (a) Intensity of the ζ-312-diffraction peak and the δ_1 330-diffraction peak (b) Thickness of the ζ phase and the δ_1 phase.

time. The thickness of the ζ phase increased in proportion to the square root of heating time. The thickness of the δ_1 phase also increased in proportion to the square root of heating time when the incubation period was taken into account. The growth rate constant of the δ_1 phase ($16.35\,\mu m^2 s^{-1}$) agreed well with that in the galvanized sample. Therefore, it is considered that these growth behaviors during the galvannealing process are dominated by the interdiffusion between Fe and Zn atoms. This behavior is consistent with the results of the measurement of iron content and thickness of the Fe-Zn intermetallic compounds in the zinc coating in published reports.[7,14)]

Figure 9 shows a comparison of growth behavior of the ζ and δ_1 phases between the coatings of 10 and 30 μm in thickness.[11)] As shown in Fig. 9(a), the growth rate of the ζ phase was independent of the thickness of the coating, and the thickness of the ζ phase saturated at 12∼13 μm in the 30 μm coating sample. On the other hand, growth behavior of the δ_1 phase depended on the thickness of the coating as shown in Fig. 9(b). The growth rate of the δ_1 phase in the 10 μm coating sample is larger than that in the 30 μm coating sample. The incubation period in the growth of δ_1 phase also depended on thickness of the coating. This suggests that existence of the ζ phase affects the growth of the δ_1 phase in the zinc coating. Figure 10 shows a relationship between the total thickness of Fe-Zn intermetallic compounds and heating time in the 10 μm and that in the 30 μm coating. The total thickness in both the coatings is plotted on the same parabola, approximately. This indicates the growth rate of the entire Fe-Zn intermetallic compounds is independent of the thickness of the coating. Therefore, the thickness of the coating contributes to the phase distribution between the ζ phase and the δ_1 phase in the Fe-Zn intermetallic compound layer. According to the binary phase diagram of Fe-Zn system, liquid zinc, ζ, δ_1 and Γ (Γ_1) phases exist on steel substrate with layered structure during the heat treatment although the Γ phase was not observed in the heating period in this experiment. Since the ζ phase has the largest interdiffusion coefficient in these compounds,[13,15–17)] it grows prior to others. It is considered that the prior growth of the ζ phase causes the delay in the growth of δ_1 phase. Furthermore, it is also considered that the concentration gradient of iron and zinc in the ζ phase influences the growth rate of the δ_1 phase.

4. Conclusions

In this study, *in-situ* observations of the growth behaviors of the Fe-Zn intermetallic compounds, the ζ and δ_1 phases, in zinc coating were performed by synchrotron radiation. The obtained results were as follows:

(1) The diffraction peak profiles were successfully obtained at intervals of 1 second with heating the sample, and the growth of the Fe-Zn intermetallic compounds was

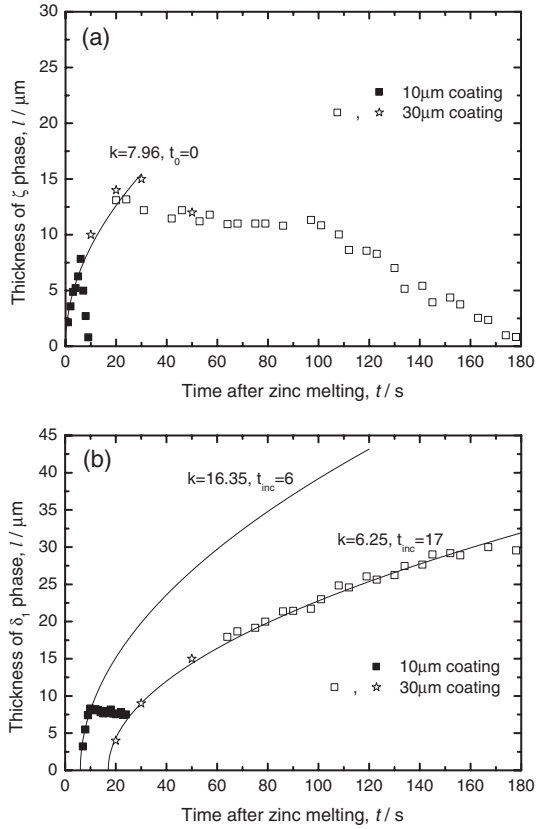

Fig. 9 Comparison of the variation of thickness of Fe-Zn intermetallic compounds between thin and thick coating in the electroplated sample. The stars show the thickness estimated with cross sectional SEM observations. (a) ζ phase (b) δ_1 phase.

observed dynamically.

(2) In the galvanized sample including 0.13 mass% Al in the coating, the diffraction peak of the ζ phase was not observed during the heat treatment. An incubation period of 7 seconds in the growth of the δ_1 phase was observed. The thickness estimated with the peak intensity of the δ_1 phase increased in proportion to the square root of heating time when the incubation period was taken into account, at the initial stage of galvannealing process.

(3) In the electroplated sample including no aluminum in the coating, the thickness of the ζ phase increased in proportion to the square root of heating time. An incubation period was also observed in the growth of the δ_1 phase, and the δ_1 phase was observed 6 seconds later after the zinc coating fully melted. The thickness of the δ_1 phase also increased in proportion to the square root of heating.

These results suggest that the growth behavior of the δ_1 phase always follows parabolic law, and is dominated by the interdiffusion between Fe and Zn, neither by interfacial reaction neither by autocatalytic reaction whether the coating contains aluminum or not, even at the initial stage of galvannealing process.

Acknowledgments

The authors thank to Dr. Ichiro Hirosawa in Japan Synchrotron Radiation Research Institute for his useful advice in the synchrotron radiation (SR) experiment. The authors thank to Mr. Hikaru Kawata in Sumitomo Metal Industries, Ltd. for his great contribution in the SR experiment and the sample preparation. The authors also thank to Mr. Tamotsu Toki and Mr. Katsuhiko Ono in Sumitomo Metal Industries, Ltd. for their help in the preparation of galvanized steel sheets. The SR experiments were performed at the SPring-8 with the approval of the Japan Synchrotron Radiation Research Institute (JASRI) (Proposal Nos. 2002A0658-NI-np and 2002B0578-NI-np).

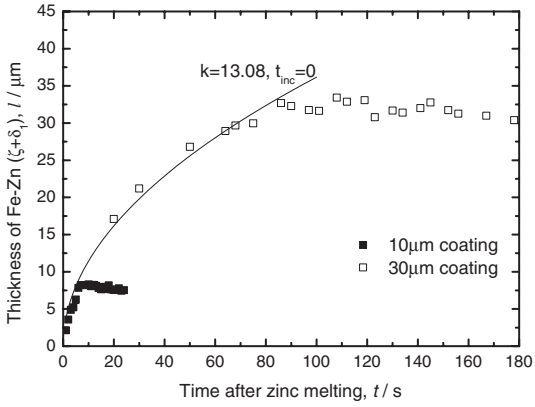

Fig. 10 Comparison of the variation of the Fe-Zn $(\zeta + \delta_1)$ thickness between thin and thick coating in the electroplated sample.

REFERENCES

1) H. Bablik, F. Gotzl and R. Kukaczka: Werkst. Korros. **2** (1951) 163–165.
2) D. Horstmann: Arch. Eisenhüttenwes. **27** (1956) 297–302.
3) A. R. Borzillo and W. C. Hann: Trans. ASM **62** (1969) 729–739.
4) E. Baril and G. L'Espérance: Metall. and Mater. Trans. A **30A** (1999) 681–695.
5) A. Nishimoto, J. Inagaki and K. Nakaoka: Tetsu-to-Hagané **72** (1986) 989–996.
6) M. Saito, Y. Uchida, T. Kittaka, Y. Hirose and Y. Hisamatsu: Tetsu-to-Hagané **77** (1991) 947–954.
7) H. Yamaguchi and Y. Hisamatsu: Trans. ISIJ **19** (1979) 649–658.
8) T. Nakamori and A. Shibuya: Tetsu-to-Hagané **77** (1991) 955–962.
9) F. Rizzo, S. Doyle and T. Wroblewski: Nucl. Instrum. Methods in Phys. Res. B **97** (1995) 479–482.
10) M. Kimura, M. Imafuku, M. Kurosaki and S. Fujii: J. Synchrotron Rad. 5 (1998) 983–985.
11) A. Taniyama, T. Takayama, M. Arai, H. Kawata, M. Sato, I. Hirosawa, T. Fukuda and J. Mizuki: Proc. of Int. Conf. on Designing of Interface Structure in Advanced Materials and their Joints (DIS'02), Osaka Japan, (2002) 385–390.
12) A. Taniyama, D. Shindo and T. Oikawa: J. Electron Microsc. **45** (1996) 232–235.
13) Syahbuddin, P. R. Munroe, C. S. Laksmi and B. Gleeson: Mater. Sci. Eng. A **251** (1998) 87–93.
14) C. E. Jordan and A. R. Marder: J. Mater. Sci. **32** (1997) 5593–5602.
15) M. Onishi, Y. Wakamatu, K. Fukumoto and M. Sagara: J. Japan Inst. Metals **36** (1972) 150–156.
16) Y. Wakamatsu, K. Samura and M. Onishi: J. Japan Inst. Metals **41** (1977) 664–669.
17) P. J. Gelling, E. W. de Bree and G. Gierman: Z. Metallkd. **70** (1979) 315–317.